

Application of direct laser metal tooling for AISI H13 tool steel

Jae-Ho LEE, Jeong-Hwan JANG, Byeong-Don JOO, Hong-Sup YIM, Young-Hoon MOON

School of Mechanical Engineering, Pusan National University, Busan 609-735, Korea

Received 2 March 2009; accepted 30 May 2009

Abstract: In the die industry, it is commonly agreed that residual tool life can be successfully extended by timely repair of damaged surfaces. Traditionally, the main repair process is tungsten inert gas (TIG) welding, but a new process called direct laser metal tooling (DLMT) emerges. DLMT is a manual process, of which results depend on the materials of the powders and tools, the laser process and parameters. This technology is a direct-metal freeform fabrication technique in which a 200 W fiber laser is used. AISI H13 tool steel is a suitable material for die casting tools because of the high resistance to thermal fatigue and dimensional stability. In this research, AISI H13 tool steel was melted with metal powder by fiber laser. Before melting AISI H13, the powders were analyzed with XRF equipment. Then, hardness distribution of laser melted zone was investigated. The microstructure in laser melted zone was discussed. In order to identify the effect of particle size of powder on the melted zone, two types of particle sizes of powders were used. Experimental results show that the mold repair process using DLMT can be applied in the mold repair industry.

Key words: direct laser metal tooling; fiber laser; AISI H13 steel

1 Introduction

Direct laser metal tooling (DLMT) is one of the few RP technologies, which possesses the capability to produce parts directly from metal powders. In fact, the process gives a great promise for direct production of functional prototypes and tools. In this method, a laser beam is scanned across the surface of a loose powder bed, melting the powders into the shape of the required cross section launched by CAD data. Therefore, it is a novel technique for producing components from various powder materials with complicated spatial forms without using conventional costly means of shaping. This processing can be applied to repairing, remodeling, and restoration of damaged mold[1–6]. Tungsten inert gas (TIG) welding is the most common process currently in use for repair welding due to great process control suited for small area, thin sections and sharp edges. This process is needed to extra stage such as grinding, milling, and heat treating before repairing and mechanical properties of after repaired mold can be fell-off[7]. DLMT is applied to overcoming the above disadvantages. It can repair a mold without additional pre-heating and post-heating. Hot-work tool steel of H13 is used in precision molds by manufacturing tools for processing or

various dies casting since it has advantages of high resistance to thermal shock, thermal fatigue, abrasion resistance, and heat resistant[8–9]. Various lasers such as CO₂ laser, Nd:YAG laser, diode laser and fiber laser have been developed for DLMT. Fiber laser has some advantages such as simplicity, high electrical to optical efficiency, reliability, excellent thermal properties, robustness, and low running cost[10–11]. In this research, melting was produced by fiber laser with various laser parameters such as laser power, scan rate, and powder particle size. Furthermore, Vickers hardness and microstructure of the melted zone were analyzed.

2 Experimental

2.1 Set up

Fig.1 shows the laser system. Fiber laser(IPG YLR-200) has wave length of 1.07 μm and its maximum power is 200 W. Laser with beam diameter of 80 μm can be applied to precision mold. And scanner (SCANLAB hurrySCAN[®] 20) is a system which controls laser scanning method. To produce oxide-free coatings in all experiments, the chamber was shielded using N₂ gas (5 L/min). Piston in the cylinder was driven by stepping actuator with the minimum step size of 10 μm. The motor was controlled through in-house software, which

also enables communication between laser and chamber to provide automation of the process.

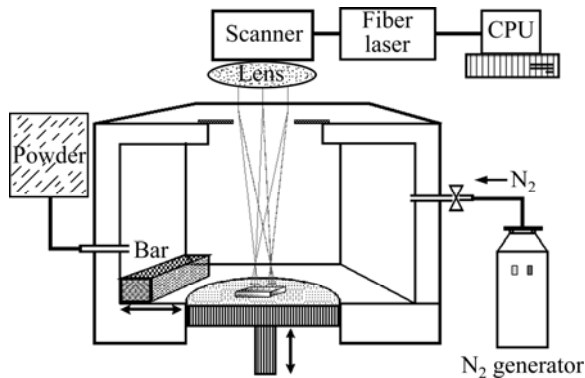


Fig.1 Schematic drawing of direct laser metal tooling system

2.2 Materials

The substrate is AISI H13 tool steel that is hot-rolled mold tool steel and widely used in the mold. The chemical composition of the substrate is listed Table 1. The powder is Fe-Ni-Cr powder with the chemical composition given in Table 1. The particle sizes are 20 and 50 μm . Fig.2 shows SEM image of 20 μm Fe-Cr-Ni powder. Particle shapes of two powders are spherical.

Table 1 Chemical composition of AISI H13 and Fe-Cr-Ni powder (mass fraction, %)

| Specimen | Fe | Cr | Ni | Mo | Si | V | Mn | C |
|-----------------|------|------|-----|------|------|-----|------|------|
| AISI H13 | Bal. | 5.2 | 1.3 | 1.23 | 1.12 | 1.1 | 0.41 | 0.41 |
| Specimen | Fe | Cr | Ni | Al | Si | S | Mn | Mo |
| Fe-Cr-Ni powder | 70.9 | 18.2 | 7.6 | 0.7 | 0.6 | 0.3 | 1.2 | 0.2 |

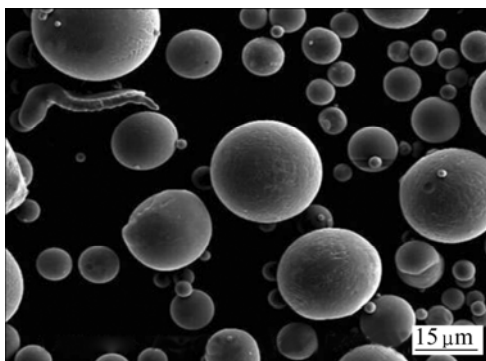


Fig.2 SEM image of 20 μm Fe-Cr-Ni powder

2.3 Experimental method

The powder layer was fabricated at a laser power of 50–200 W and a scan rate of 33.6–439.2 mm/s. Other process parameters used in the experiment are listed in Table 2. Surface properties that mainly result in layer

properties were measured through the single layer scanning experiment. In order to fabricate multiple layer, optimized process parameters were used. The layered specimens were 10 mm in length and 10 mm in width. Vickers hardness and microstructure of the melted zone were analyzed according to the distance from base metal.

Table 2 Conditions of experiment

| Parameter | Value |
|---|-------------------|
| Power/W | 50, 100, 150, 200 |
| Scan rate/($\text{mm}\cdot\text{s}^{-1}$) | 36.6–439.2 |
| Particle size/ μm | 20, 50 |
| Fill spacing/ μm | 60 |
| Beam size/ μm | 80 |

3 Results and discussion

3.1 Surface behaviors under various laser conditions

Fig.3 shows schematic drawing of three different surface patterns. The pattern that has balling and rough surface is defined as Type I, well connected pattern that has fine surface is defined as Type II. Type III is the unconnected pattern.

Ranges of Type II can be used to build next step. Ranges of Type I and Type III are not used to layer next step anymore. Type I is observed with power increasing and scan rate decreasing. Type III is observed with opposite conditions to Type I. Fig.4 shows the surface behavior diagrams at various laser powers and scan rates. The results suggest that Type I can be avoided by lowering laser power and increasing scan rate. And Type III can be avoided opposite to Type I.

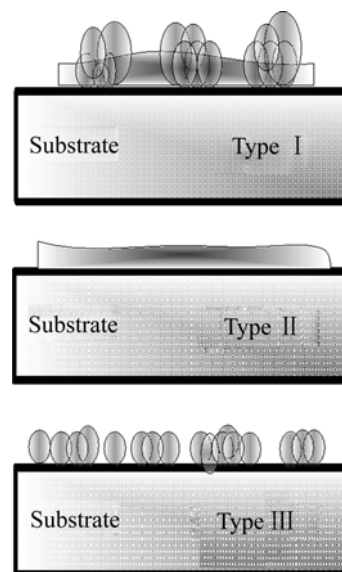


Fig.3 Schematic drawings of three different surface patterns

When the particle size is 20 μm , Type II can be obtained at scan rates of 36.6–439.2 mm/s with power control and particle size of 50 μm , and the range of scan rate that can obtain Type II is 36.6–329.4 mm/s. As the particle size increases, ranges of Type II decrease since bigger particle is needed more energy density to obtain smooth surface. 20 μm powder has wide ranges of smooth surface at 100 W laser power. On the other hand, smooth surface nearly cannot be obtained from 50 μm powder at 100 W laser power. Smaller particle size powder is more efficient than bigger particle size powder to repair mold at lower laser power.

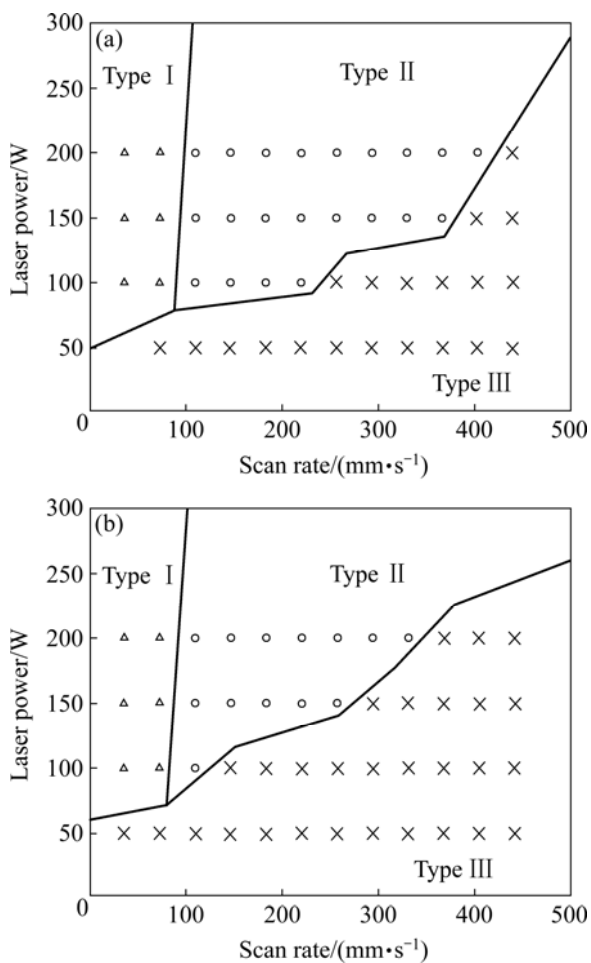


Fig.4 Process window for various laser parameters: (a) 20 μm ; (b) 50 μm

3.2 Properties of multiple layered specimens

Optimized process parameters were used to build multiple layered specimens. In order to make smooth surface, two powders were melted at different scan rates and 200 W laser power. 20 μm and 50 μm powders were melted at 219.6 and 146.4 mm/s, respectively. Fig.5 shows Vickers hardness distribution of the melted zone according to distance from base metal. Near base metal

the melted zone structure is observed like martensite structure. Its hardness is measured as very high as HV 450 and Vickers hardness of the melted zone near surface is about HV 270. Base metal structure is not affected by laser beam and hardness is about HV 230. And hardness of specimen made from 50 μm powder is higher than that of 20 μm powder. When fabricating layered specimen, 50 μm powder needs more input energy to obtain smooth surface. As the distance from base metal increases, Vickers hardness of the melted zone decreases since the early layer thickness is thinner than the latter layer thickness. Therefore, more input energy in the early layered zone is absorbed as high input energy and cooling rate increases. This phenomenon causes martensite structure in the melted zone. The melted zone microstructures according to distance from base metal are shown in Fig.6. Dense martensite structure is observed near base metal melted zone.

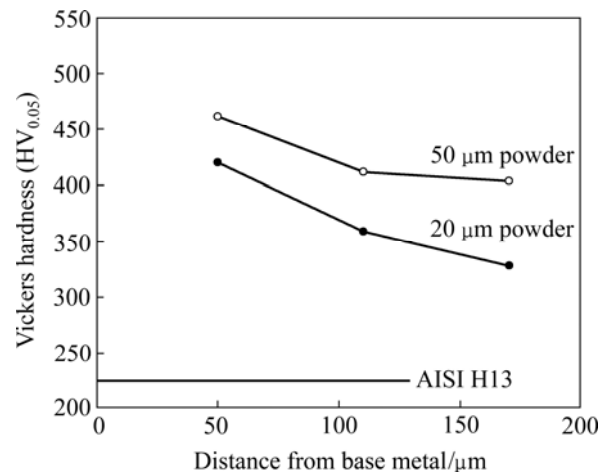


Fig.5 Vickers hardness distribution according to distance from base metal

4 Conclusions

1) Fe-Ni-Cr layer was fabricated on AISI H13 tool steel by fiber laser with various laser parameters. Surface behavior properties were measured and Vickers hardness and microstructure of melted specimens were analyzed.

2) Balling can be avoided by lowering laser power and increasing scan rate, and no connection can be avoided opposite to balling. As the particle size increases, more input energy is needed to obtain smooth surface.

3) Vickers hardness of near base metal melted zone is higher than that of near surface melted zone since near base metal melted zone has dense martensite microstructure.

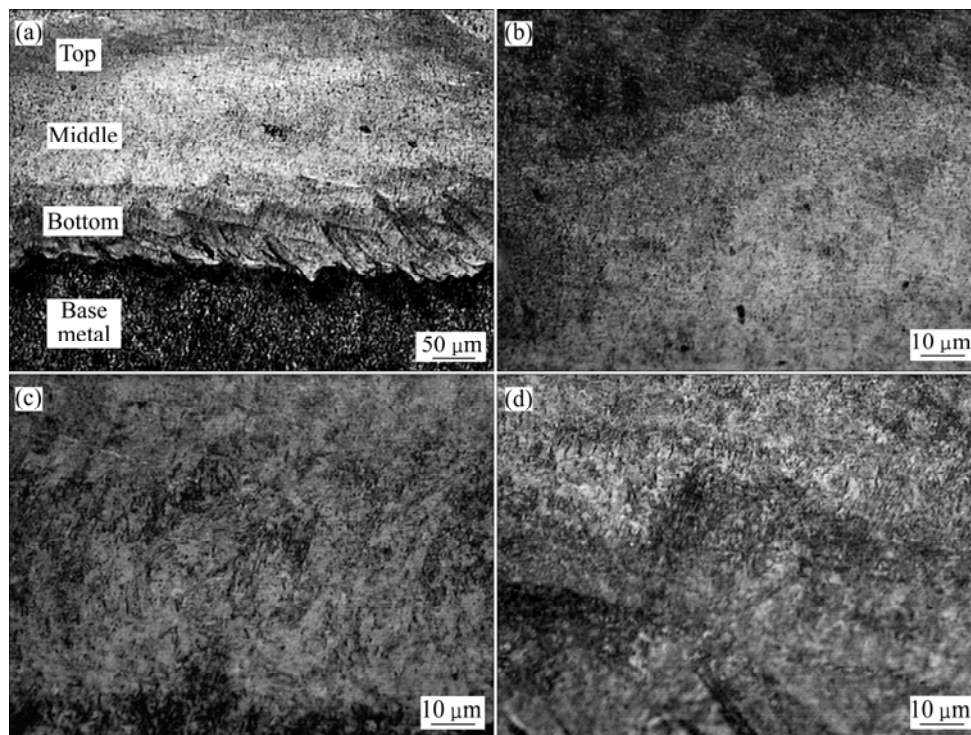


Fig.6 Microstructures of melted zone according to distance from base metal: (a) Melted zone; (b) Top of melted zone; (c) Middle of melted zone; (d) Bottom of melted zone

Acknowledgement

This work is partially supported by the Korea Research Foundation Grant funded by the Korean Government (MOEHRD, Basic Research Promotion Fund) and Grants-in-aid for the National Core Research Center Program from MOST/KOSEF.

References

- [1] SONG R, HANAKI S, YAMASHITA M, UCHIDA H. Reliability evaluation of a laser repaired die-casting die[J]. *Mater Sci Eng A*, 2008, 483/484: 343–345.
- [2] SIMCHI A, POHL H. Effects of laser sintering processing parameters on the microstructure and densification of iron powder[J]. *Mater Sci Eng A*, 2003, 359: 119–128.
- [3] VEDANI M. Microstructural evolution of tool steels after Nd-YAG laser repair welding[J]. *Journal of Materials Science*, 2004, 39: 241–249.
- [4] VEDANI M, PREVITALI B, VIMERCATI G M, SANVITO A, SOMASCHINI G. Problems in laser repair—Welding a surface-treated tool steel[J]. *Surface and Coatings Technology*, 2007, 201: 4518–4525.
- [5] JENG J Y, LIN M C. Mold fabrication and modification using hybrid processes of selective laser cladding and milling[J]. *Journal of Materials Processing Technology*, 2001, 110: 98–103.
- [6] YADROITSEV I, BERTRAND P H, SMUROV I. Parametric analysis of the selective laser melting process[J]. *Applied Surface Science*, 2007, 253: 8064–8069.
- [7] WANG X C, LAOUI T, BONSE J, KRUTH J P, LAUWERS B, FROYEN L. Direct selective laser sintering of hard metal powders: Experimental study and simulation[J]. *Advanced Manufacturing Technology*, 2002, 19: 351–357.
- [8] MAEDA K, CHILDS T H C. Laser sintering (SLS) of hard metal powders for abrasion resistant coatings[J]. *Journal of Materials Processing Technology*, 2004, 149: 609–615.
- [9] SHIN H J, YOO Y T, AHN D G, SHIN B H. The surface heat treatment of die steel SKD61 using CW Nd:YAG laser[C]//Proceeding of KSME 2006 Spring Annual Meeting. 2006: 3080–3085.
- [10] HAN Y H. Laser beam quality and process efficiency[C]//Proceeding of Korea Society of Laser Processing, 2006 Spring Annual Meeting. 2006: 48–50.
- [11] KAWAHITO Y, TERAJIMA T, KIMURA H, KURODA T, NAKATA K, KATAYAMA S, INUOUE A. High-power fiber laser welding and its application to metallic glass $Zr_{55}Al_{10}Zr_{15}Cu_{30}$ [J]. *Mater Sci Eng B*, 2008, 148: 105–109.

(Edited by CHEN Wei-ping)